

# Preparation of PFS coagulant by sectionalized reactor

CHANG Qing\*, WANG Hong-yu

(Department of Environmental Engineering, Lanzhou Railway College, Lanzhou 730070, China. E-mail: changq@lzri.edu.cn)

**Abstract:** The oxidation rate of ferrous sulfate is investigated for the preparation of polyferric sulfate (PFS) coagulant. It is proved that this reaction is zero order with respect to  $\text{Fe}^{2+}$ , first order with respect to  $\text{NO}_2(\text{g})$ , and first order with respect to the interface area between gas phase and liquid phase. According to this mechanism, sectionalized reactor (SR) is used in place of traditional reactor (TR), and the liquid of reaction mixture is recycled by pump. As a result, not only the flow path of reaction liquid is prolonged, but also gas-liquid contact area enlarged, and the reaction distinctly accelerated, compared with traditional reactor. The effects of parameters including temperature, acidity and others on the reaction rate are also discussed.

**Keywords:** coagulant; flocculant; polyferric sulfate; PFS; oxidation rate; water treatment

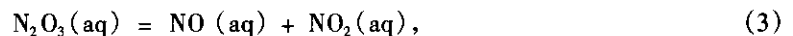
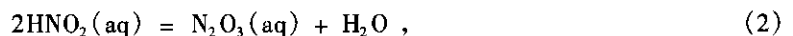
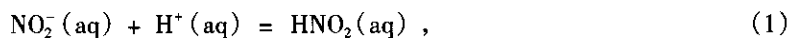
## Introduction

Polyferric sulfate (PFS) is a sort of inorganic coagulant with high molecular weight. The general formula is  $[\text{Fe}_2(\text{OH})_n(\text{SO}_4)_{3-0.5n}]_m$  ( $n < 2$ ,  $m > 10$ ) (Chang, 1993). It contains polynuclear complex ions such as  $\text{Fe}_2(\text{OH})_2^{4+}$ ,  $\text{Fe}_3(\text{OH})_4^{5+}$  formed by OH bridge and a large quantity of inorganic macromolecular compounds. The molecular weight can be as high as  $10^5$  (Spiro, 1966). These constituents can be adsorbed by colloidal particles so that the surface charge of colloids and suspended substances is neutralized, so the colloidal particles and suspended substances change from repelling each other to attracting each other, then collide and precipitate as large aggregates. Because these large aggregates have very large surface area with excellent adsorption capacity, PFS is more effective than any other inorganic coagulants for removing COD, BOD, color and dissolved organic matter from natural water or waste water. In addition, PFS is very efficient within wider ranges of temperature and pH value because of its strong hydrolysis. So it can be used under low-temperature conditions.

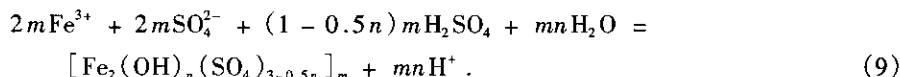
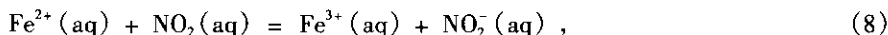
A preparation method of PFS coagulant from  $\text{FeSO}_4$  was reported by Japanese scientists in the 1970's (Shigeo, 1978; Mikami, 1980). Today, it is still a practicable method because the materials used in this method are very cheap. In this method, iron in a ferrous state is oxidized to ferric state when using  $\text{O}_2$  as the oxidant and  $\text{NaNO}_2$  as the catalyst. After this oxidation, the partial hydrolysis and polymerization of ferric iron are followed. Since the 1980's, the preparation and application of PFS have been widely investigated in China (Yang, 1986; Chen, 1995; Li, 1995; 1998; Bai, 1996; Chang, 2001) and other countries (Tang, 1987a; 1987b; Jiang, 1993; 1998) because of its high coagulation performance in water treatment. But so far the mechanism of the preparation has not been properly understood, as a result, now the time needed to complete the preparation is still too long. In order to shorten the preparation time and consider the scientific relevance, the reaction kinetics and the technological process are investigated.

## 1 Mechanism of preparation

### 1.1 The equations of reaction



\* Corresponding author



Where  $\text{NaNO}_2$  acts as the catalyst in these reactions. Eqs. (1)—(3) show that  $\text{NaNO}_2$  reacts with  $\text{H}^+$  producing  $\text{NO}_2$  and  $\text{NO}$  when it is added to the solution. The produced  $\text{NO}$  in the solution enters gas phase and is oxidized by  $\text{O}_2$  becoming  $\text{NO}_2$ , as shown in Eqs. (4)—(6). The produced  $\text{NO}_2$  in the gas phase again enters liquid phase and oxidizes  $\text{Fe}^{2+}$  to  $\text{Fe}^{3+}$ , as shown in Eqs. (7)—(8). The  $\text{NO}_2^-$  produced in Eq. (8) repeats reactions (1)—(8), continuing the oxidation of  $\text{Fe}^{2+}$  to  $\text{Fe}^{3+}$ . Eq. (9) shows that the produced  $\text{Fe}^{3+}$  partially hydrolyzes and polymerizes becoming product PFS at last because the added sulfuric acid is not enough for ferric sulfate to form.

## 1.2 The transfer rate of $\text{NO}_2$

The rate equation of the transfer can be deduced by a "double membrane model" which is shown in Fig. 1. From this figure it can be seen that  $C$  is the concentration of  $\text{NO}_2$  in the main body of the gas phase or the liquid phase;  $C'$  is the concentration of  $\text{NO}_2$  in the boundary layers. Because of turbulence in the gas phase and stir in the liquid phase, the concentration of  $\text{NO}_2$  is uniform everywhere in the main bodies, but it decreases along the transfer direction in the boundary layers. When the transfer takes place,  $\text{NO}_2(\text{g})$  first enters the gas boundary layer, then passes through the liquid boundary layer, finally comes into the liquid main body. Because  $\text{NO}_2$  transfers by means of diffusion in the boundary layers, the first Fick's law of diffusion is followed:

$$J_g = -D_g A [dC_{\text{NO}_2(\text{g})}/dX_g] = D_g A [C_{\text{NO}_2(\text{g})} - C'_{\text{NO}_2(\text{g})}]/X_g, \quad (10)$$

$$J_l = -D_l A [dC_{\text{NO}_2(\text{aq})}/dX_l] = D_l A [C'_{\text{NO}_2(\text{aq})} - C_{\text{NO}_2(\text{aq})}]/X_l, \quad (11)$$

where  $J_g$  and  $J_l$  are the transfer rate of  $\text{NO}_2$ ,  $D_g$  and  $D_l$  are the diffusion coefficients of  $\text{NO}_2$ ,  $X_g$  and  $X_l$  are the thickness of the boundary layers, respectively in the gas boundary layer and the liquid boundary layer,  $A$  is the interface area. If Henry's law is followed, we will have  $C'_{\text{NO}_2(\text{g})} = HC'_{\text{NO}_2(\text{aq})}$  and  $C_{\text{NO}_2(\text{g})} = HC_{\text{NO}_2(\text{aq})}^*$ , here  $H$  is Henry constant,  $C_{\text{NO}_2(\text{aq})}^*$  is the concentration of  $\text{NO}_2(\text{aq})$  in the liquid main body when it is in equilibrium with  $\text{NO}_2(\text{g})$  in the gas main body, and if the transfer reaches a stable state,  $J = J_g = J_l$ , so Equations (10) and (11) become:

$$J = D_g A [HC_{\text{NO}_2(\text{aq})}^* - HC'_{\text{NO}_2(\text{aq})}]/X_g, \quad (12)$$

$$J = D_l A [C'_{\text{NO}_2(\text{aq})} - C_{\text{NO}_2(\text{aq})}]/X_l. \quad (13)$$

Or

$$JX_g/D_gAH = C_{\text{NO}_2(\text{aq})}^* - C'_{\text{NO}_2(\text{aq})}, \quad (14)$$

$$JX_l/D_lA = C'_{\text{NO}_2(\text{aq})} - C_{\text{NO}_2(\text{aq})}. \quad (15)$$

By summation of (14) and (15), and by substituting  $C'_{\text{NO}_2(\text{g})}/H$  for  $C_{\text{NO}_2(\text{aq})}^*$  we have:

$$J = D_g D_l A [C_{\text{NO}_2(\text{g})} - C_{\text{NO}_2(\text{aq})}]/[X_g D_l + X_l D_g H]. \quad (16)$$

Since the solution was strongly stirred,  $X_l$  is very small and  $X_l D_g H$  can be neglected, Equation (16) becomes:

$$J = D_g A [C_{\text{NO}_2(\text{g})} - HC_{\text{NO}_2(\text{aq})}]/X_g. \quad (17)$$

It can be seen that the larger interface area is, the more quickly  $\text{NO}_2$  transfers across the interface,

the higher partial pressure of  $\text{NO}_2(\text{g})$  is and the more quickly  $\text{NO}_2$  transfers across the interface.

**1.3 The concentration of  $\text{NO}_2$  in the solution**

As soon as  $\text{NO}_2(\text{g})$  enters the solution, it quickly reacts with  $\text{Fe}^{2+}$ . The concentration of  $\text{NO}_2(\text{aq})$  in the solution can be obtained by stable state treatment:

$$\begin{aligned} dC_{\text{NO}_2(\text{aq})}/dt &= J - VK_8 C_{\text{Fe}^{2+}} C_{\text{NO}_2(\text{aq})} = \\ D_g A [C_{\text{NO}_2(\text{g})} - HC_{\text{NO}_2(\text{aq})}] / X_g - \\ VK_8 C_{\text{Fe}^{2+}} C_{\text{NO}_2(\text{aq})} &= 0, \end{aligned} \tag{18}$$

where  $V$  is the volume of the solution,  $K_8$  is the reaction rate constant of Eq. (8). From Eq. (18), following equation is obtained:

$$C_{\text{NO}_2(\text{aq})} = D_g AC_{\text{NO}_2(\text{g})} / [X_g (D_g AH / X_g + VK_8 C_{\text{Fe}^{2+}})].$$

Because the gas phase was not stirred,  $X_g$  is relatively large. So  $D_g AH / X_g$  can be neglected, therefore we have

$$C_{\text{NO}_2(\text{aq})} = D_g AC_{\text{NO}_2(\text{g})} / X_g VK_8 C_{\text{Fe}^{2+}}. \tag{19}$$

**1.4 The rate equations of the reaction**

According to Eq. (8), the oxidation rate of  $\text{Fe}^{2+}$  is expressed as following:

$$-dC_{\text{Fe}^{2+}}/dt = K_8 C_{\text{Fe}^{2+}} C_{\text{NO}_2(\text{aq})}. \tag{20}$$

By substituting Equation (19) for  $C_{\text{NO}_2(\text{aq})}$  in Equation (20), we have

$$-dC_{\text{Fe}^{2+}}/dt = D_g AC_{\text{NO}_2(\text{g})} / (X_g V) = KAC_{\text{NO}_2(\text{g})}, \tag{21}$$

where  $K = D_g / (X_g V)$ . It is clear that this reaction is zero order with respect to  $\text{Fe}^{2+}$ , first order with respect to  $\text{NO}_2(\text{g})$ , and first order with respect to interface area  $A$ . So in order to reduce the time needed to complete the reaction, the pressure of  $\text{NO}_2(\text{g})$  can be increased (it was experimentally proved in Fig. 6), but this will make the corrosion of devices more serious, and the pressure resisting devices are to be adopted. Also the interface area between gas phase and liquid phase can be increased to reduce the reaction time.

If the  $C_{\text{NO}_2(\text{g})}$  and the interface area  $A$  are kept constant, Equation (21) becomes:

$$-dC_{\text{Fe}^{2+}}/dt = K, \tag{22}$$

the integral equation will be:

$$C_{\text{Fe}^{2+}} = -Kt + B, \tag{23}$$

where  $B$  is the integral constant. It shows  $\text{Fe}^{2+}$  decrease linearly with time. This is also proved by our experiment (Fig.4).

From above discussions and Equation (21), it is concluded that the transfer of  $\text{NO}_2$  from gas phase to liquid phase is the key procedure and the gas-liquid interface area is an important factor which controls the rate of the whole process.

**2 Experiment**

**2.1 Devices and process flow diagram for preparation of PFS**

PFS was prepared by using the devices of traditional reactor (TR) and sectionalized reactor (SR) respectively, as shown in Fig.2 and Fig.3. The reactor volume is  $1.5 \text{ dm}^3$  both for TR and for SR. When TR is used, the liquid of reaction mixture is strongly stirred by a stirrer; but when SR is used, the liquid of reaction mixture is recycled at a flow rate of 5 L/h by a wriggle pump during the whole process to prolong

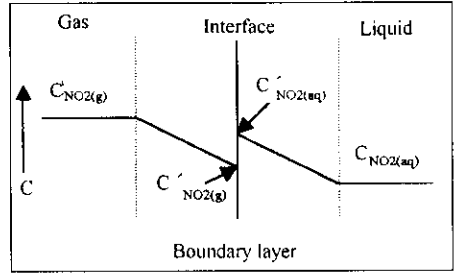


Fig.1 Double membrane model

the flow path of reaction liquid and enlarge the gas-liquid contact area.

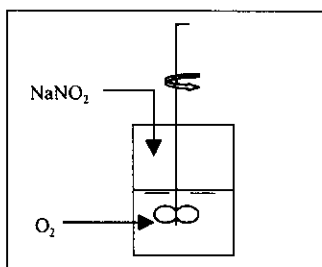


Fig. 2 Traditional reactor

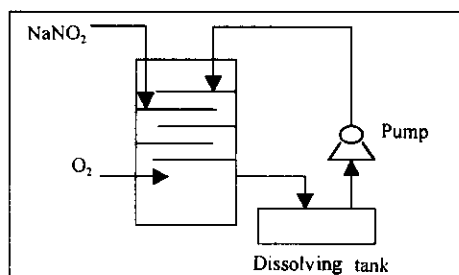


Fig. 3 Sectionalized reactor

## 2.2 Experimental methods and procedures

The total amount of 324g  $\text{FeSO}_4 \cdot 7\text{H}_2\text{O}$  was added to the reactor (TR or SR), but first only 162g  $\text{FeSO}_4 \cdot 7\text{H}_2\text{O}$  along with 170 ml  $\text{H}_2\text{O}$  and 22 ml  $\text{H}_2\text{SO}_4$  (95%—98%) were added because the solubility of  $\text{FeSO}_4 \cdot 7\text{H}_2\text{O}$  is limited. Then the solution of  $\text{NaNO}_2$  was slowly added to the reactor from the top of the reactor by a dropping funnel while pure oxygen was being conducted to the reactor from the bottom of the reactor, as shown in Fig. 2 and Fig 3. In the following process, the remaining  $\text{FeSO}_4 \cdot 7\text{H}_2\text{O}$  (162g) was added in batches, once every 5—10 minutes, until the addition of total amount of  $\text{FeSO}_4 \cdot 7\text{H}_2\text{O}$  was finished. During the whole reaction process, temperature was maintained at 50—60°C, and pressure was controlled at  $101325 \pm 666.6$  Pa by a gas receiver and a pressure gauge, and the reaction was carried out under hermetic condition. The solution in the reactors was sampled at intervals, and the total iron (III + II) was determined by potassium dichromate method, and the ferric iron by iodimetric method, and the ferrous iron by potassium permanganate method respectively. When all  $\text{Fe}^{2+}$  was oxidized to  $\text{Fe}^{3+}$ , the solution turned red brown. The reaction was ended. The viscosity of the product was measured by ubbelohde viscometer; and the hydrolysis of the product was measured by neutralization method; and the density of the product was measured by densimeter; and the pH value of the product was measured by acidimeter respectively.

## 3 Results and discussions

### 3.1 The properties of the product

The properties of the product are shown in the following table.

Table 1 The properties of the product

pH	Density, g/ml	$\text{Fe}^{2+}$ , g/L	$\text{Fe}^{3+}$ , g/L	Hydrolysis, $[\text{OH}]/3[\text{Fe}]$	Viscosity, cp
0.5	1.44	0.16	162	16%	11

It can be seen that the product fulfills the China National Standard Class A.

### 3.2 Comparison between SR and TR

Ferrous iron linearly decreases with time no matter what kind of reactor is used as shown in Fig. 4. This result accords with the Eq. (23), which proves the above oxidation rate theory and the rate equations of reaction proposed by us.

The comparison of reaction rate between SR and TR is also shown in Fig. 4. When TR is used, the renewal of liquid surface is made by stirring. Because of limiting stirring rate and small gas-liquid contact area, the reaction is very slow that the time needed to complete the reaction is more than ten hours. But when SR is used, the gas-liquid contact area is enlarged, and the transfer of  $\text{NO}_2$  between gas-liquid interface is accelerated, so that the time needed to complete the reaction is cut down to 2-3 hours, again, this proves the theory and rate equation proposed by us.

### 3.3 Effect of temperature on reaction rate

As from Fig.5, the time needed to complete reaction decreases when temperature is raised within the range from 25°C to 50°C. But temperature make little difference to reaction rate when it is above 50°C. When temperature is above 80°C, hydrolysis of the polymer is rather serious, so the yellow precipitant of Fe(OH)SO<sub>4</sub> forms readily. Therefore the optimum temperature should be controlled at 50°C.

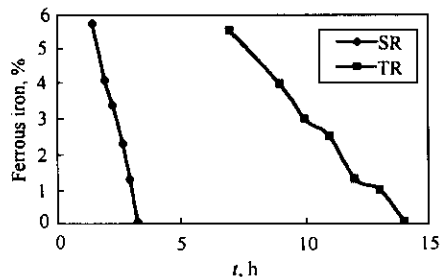


Fig.4 Comparison of reaction rate

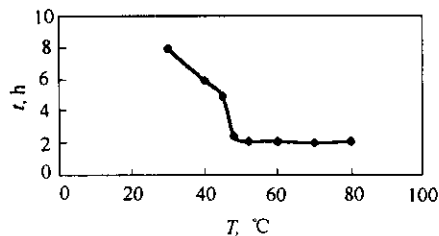


Fig.5 Relation between temperature and reaction time

### 3.4 Effect of NaNO<sub>2</sub> addition rate on reaction rate

The solution of NaNO<sub>2</sub> was dropped at intervals into SR during the entire reaction process. When the addition rate of NaNO<sub>2</sub> solution is higher, the partial pressure of NO<sub>2</sub>(g) is higher, and the ferrous iron more quickly changes to ferric iron, so the concentration of Fe<sup>2+</sup> more quickly decreases as seen from Fig. 6. This result accords with the Eq.(21), which proves the theory and rate equation proposed above. It can be found that not only the change is slow, but also the total consumption of NaNO<sub>2</sub> is higher when the solution of NaNO<sub>2</sub> is dropped slowly. So the addition rate of NaNO<sub>2</sub> solution should not be too low.

### 3.5 Effect of acidity on reaction rate

The electrode potential for Fe<sup>3+</sup>/Fe<sup>2+</sup> is strongly depending on the acidity (or basicity) of the solution, which can be shown as follows:

in acid solution:  $\phi^{\theta}(\text{Fe}^{3+}/\text{Fe}^{2+}) = 0.771\text{V}$  ;

in basic solution:  $\phi^{\theta}(\text{Fe}^{3+}/\text{Fe}^{2+}) = -0.56\text{V}$  .

Therefore, when pH value of the solution is lower, Fe<sup>2+</sup> is more stable than Fe<sup>3+</sup>, and the former can not be easily oxidized; when pH value of the solution is higher,

Fe<sup>3+</sup> is more stable than Fe<sup>2+</sup>, and the latter can be readily oxidized. So pH value should be as high as possible for changing Fe<sup>2+</sup> into Fe<sup>3+</sup>. But there is a limit because excessively high pH value can cause intense hydrolysis of Fe<sup>3+</sup> and result in the formation of Fe(OH)SO<sub>4</sub> precipitant. Usually pH value should be lower than 1.6. To cope with this problem, both FeSO<sub>4</sub>·7H<sub>2</sub>O and concentrated sulfuric acid should be added in batches to decrease the concentration of Fe<sup>2+</sup> and concentrated sulfuric acid in the solution.

### 3.6 Effect of the ratio of total SO<sub>4</sub><sup>2-</sup> to total Fe on product viscosity

It was noticed that the ratio of total SO<sub>4</sub><sup>2-</sup> to total Fe affects the viscosity of the product. Viscosity increases as the ratio is raised, as seen from Table 2. Yellow precipitant readily forms when the viscosity is too high, therefore, the ratio of total SO<sub>4</sub><sup>2-</sup> to total Fe should be controlled carefully.

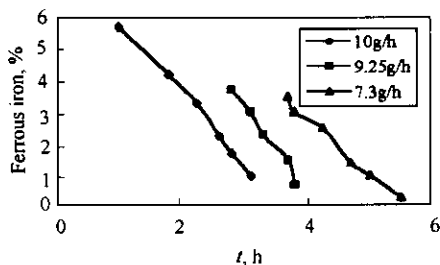


Fig.6 Effect of NaNO<sub>2</sub> addition rate on reaction rate

Table 2 The effect of SO<sub>4</sub><sup>2-</sup> on the viscosity

No	ΣSO <sub>4</sub> <sup>2-</sup> (mol)/ΣFe(mol)	Viscosity, cp
1	1.20	11.8
2	1.25	13.4
3	1.30	14.8
4	1.35	15.3

## 4 Conclusions

The oxidation of ferrous sulfate is zero order with respect to  $\text{Fe}^{2+}$ , first order with respect to  $\text{NO}_2(\text{g})$ , and first order with respect to the interface area between gas phase and liquid phase.

The transfer of  $\text{NO}_2(\text{g})$  across the interface between gas phase and liquid phase is the key procedure in the oxidation reaction of  $\text{Fe}^{2+}$  by oxygen. So sectionalized reactor was employed in place of traditional reactor and liquid of reaction mixture was recycled by pump to enlarge the gas-liquid contact area. As a result, the reaction was accelerated distinctly.

The reaction is accelerated when the temperature is raised, but too high temperature not only makes little difference to reaction rate, but also hastens the formation of precipitant. So the temperature should be controlled at  $50 \pm 2^\circ\text{C}$ .

The reaction is accelerated when the pH value is raised, but too high pH value makes precipitant form readily. So the pH value should be controlled lower than 1.6.

Not only the reaction rate is lower but also the total consumption of  $\text{NaNO}_2$  is higher when the solution of  $\text{NaNO}_2$  is dropped more slowly. So the addition rate of  $\text{NaNO}_2$  solution should not be too low.

## References:

- Bai Y X, Liu J, Li Y, 1996. Study on the catalyst for the preparation of PFS[J]. *Water Treatment for Industry*, 2:9—11.
- Chang Q, 1993. The principle of flocculation[M]. Lanzhou University Press. 172—175.
- Chang Q, 2001. Oxidation rate in the preparation of polyferric sulfate coagulant[J]. *J Environ Sci*, 13(1): 104—107.
- Chen F J, Li F T, Du X R, 1995. Study on the new technology for the preparation of PFS[J]. *China Water Supply and Drainage*, 11(1): 42—44.
- Jiang J Q, Graham N J D, Harward C, 1993. Comparison of polyferric sulfate with other coagulant for the removal of algae and algal-derived organic matter[J]. *Wat Sci and Tech*, 27(11): 221—229.
- Jiang J Q, Graham N J D, 1998. Preparation and characterization of optimal polyferric sulfate(PFS) as a coagulant for water treatment[J]. *J Chem Technol Biotechnol*, 73:351—358.
- Li F T, 1998. The new technology for preparation of PFS by oxidation with catalyst in foreign countries[J]. *Water Treatment for Industry*, 9: 9—10.
- Li X J, 1995. The new technology for production of PFS[J]. *Water Treatment for Industry*, 1:5—6.
- Mikami Hassuka *et al.*, 1980. The polyferric coagulant[J]. *PPM*, 11(5): 24.
- Spiro T G, Allerton S E, Renner J *et al.*, 1966. The hydrolytic polymerization of iron(III)[J]. *J Am Chem Soc*, 88:2721—2726.
- Shigeo Ban, 1978. Inorganic high MW coagulant[J]. *Water Supply for Industry*, (232):53.
- Tang H X, Stuum W, 1987. The coagulating behaviors of Fe(III) polymeric species-I[J]. *Water Res*, 21(1): 115—121.
- Tang H X, Stuum W, 1987. The coagulating behaviors of Fe(III) polymeric species-II[J]. *Water Res*, 21(1): 123—128.
- Yang B L, Qiu Zh T, Li M J, 1986. Study on the preparation of new coagulant PFS using by-product  $\text{FeSO}_4$  and waste  $\text{H}_2\text{SO}_4$  [J]. *The Technology for Purification of Water*, 3: 15—18.

(Received for review April 23, 2001. Accepted July 2, 2001)